Scale-Adaptive Simulation with Artificial Forcing

F.R. Menter, A. Garbaruk, P. Smirnov, D. Cokljat, and F. Mathey

Abstract. The present paper describes first efforts carried out to extend the range of Scale-Adaptive Simulation (SAS) methods into the area of RANS-stable flows. Instead of relying on inherent flow instabilities for generating resolved turbulence in unstable regimes, the current approach employs forcing terms for transferring modelled turbulence energy into resolved energy in pre-specified regions of the simulation domain.

1 Introduction

In recent years there was a strong drive for including unsteady elements into established RANS turbulence models. The most prominent example is the Detached Eddy Simulation (DES) approach of Spalart and co-workers (Spalart 2000) in its multiple forms. The underlying assumption of DES was to avoid the high resolution demands of Large Eddy Simulation (LES) in wall bounded flows by keeping established RANS models active there, while at the same time switching to LES-like formulations in large separation ("detached") zones. The switching is achieved by comparing the RANS and (a suitably defined) LES length scale (or the eddy-viscosity) and selecting the smaller of both. In addition, shielding functions are introduced for preserving the RANS model inside the boundary layer. The idea behind the DES methodology was essentially that RANS (or more precisely URANS) models are not capable of resolving turbulent structures in separated flow regions. This is based on the observation that standard RANS models provide only very large scale unsteady structures in unstable flows like flow past a cylinder. This behaviour is often associated with the Reynolds averaging technique underlying SAS model formulations.

F.R. Menter
ANSYS Germany GmbH, Staudenfeldweg12, 83624 Otterfing, Germany
florian.menter@ansys.con

A. Garbaruk · P. Smirnow
NTS, Russia

D. Cokljat
ANSYS, U.K.

F. Mathey
Air Liquide, France (formerly ANSYS France)

S.-H. Peng et al. (Eds.): Progress in Hybrid RANS-LES Modelling, NNFM 111, pp. 235–246.
springerlink.com

In a series of publications, Menter and Egorov (2004, 2005a, 2005b, 2005c, 2006) have demonstrated that this behaviour of RANS models is not a result of the Reynolds averaging, but of the specifics of model formulations within the RANS concept. It was shown that URANS models show entirely different unsteady characteristics when basing the scale-equation on an exact transport equation for the turbulent length scale (Rotta, 1972). This introduces the von Karman length scale into the system, which allows the model to adjust its behaviour to resolved scales. The resulting modelling concept was termed Scale-Adaptive Simulation (SAS) and it has been demonstrated that SAS models behave in many flows similarly to DES, but with less explicit impact of the grid spacing on the model formulation. Industrial experience (e.g. Grahs and Othmer, 2006, Widenhorn et al. 2009) over the last few years has shown that numerous inherently unstable flows can be handled well with the SAS formulation.

In order to produce unsteady structures, both DES and SAS rely in their classical formulation on “strong enough” flow instabilities. Such instabilities are typically observed for flows around blunt obstacles (cylinders, buildings, stalled airfoils/wings, mixers, …) or flows with a strong swirl instability (combustion chambers etc.). However, there are also many flows, where the instability is not strong enough and no, or “insufficient” unsteadiness is produced (Davidson, 2006). For DES models, this results in the well known “grey areas”, where the model switches to LES, but the flow is not sufficiently resolved and the model behaviour is undefined. In SAS, the result is a steady state RANS, or a low-fidelity URANS solution.

In order to extend the SAS approach to flows which do not exhibit a sufficiently strong instability for generating LES content, an explicit transfer of turbulent kinetic energy, k, is needed. This can be achieved with forcing terms in the momentum equations, which convert modelled k into resolved k.

The idea of forcing consists in introducing a volume stochastic source term (velocity fluctuations based on a modified Random Flow Generator (RFG) of Smirnov et al., 2001, Batten et al., 2004) in the momentum equations and a corresponding sink term in the k-transport equation of the SST-based SAS model. These terms are introduced in a confined user-specified flow region (“forcing zone”), where switching from RANS to LES mode is desired. In this zone, RFG generates unsteady structures which the SAS can then detect. The SAS model thereby automatically reduces its length scale (and eddy-viscosity) to these structures resulting in an LES-like formulation. The RFG, in turn, adapts its synthetic length sales to these smaller structures, which ultimately results in an automatic effective deactivation of the RFG in the most of the specified region. As a result, the RFG remains active only in a close vicinity of the user-specified boundary of the forcing zone. The forced SAS model will be termed SAS-F model.

2 Model Formulation

2.1 SST-SAS Model

The underlying model is the SST-SAS model which consists of the original SST model (Menter, 1994) plus an additional term in the ω–equation:

$$Q_{SAS} = \max\left[\rho\zeta_2 S^2\left(\frac{L}{L_{vK}}\right)^2 - C_{SAS}\frac{2\rho k}{\sigma_\Phi}\max\left(\frac{1}{k^2}\frac{\partial k}{\partial x_j}\frac{\partial k}{\partial x_j},\frac{1}{\omega^2}\frac{\partial \omega}{\partial x_j}\frac{\partial \omega}{\partial x_j}\right),0\right] \quad (1)$$

with $\zeta_2=1.47$, $\sigma_\Phi=2/3$ and $C_{SAS}=2$ and:

$$L_{vK} = \kappa\left|\frac{U'}{U''}\right|; \quad L = c_\mu^{-1/4}\frac{\sqrt{k}}{\omega}; \quad U'' = \sqrt{\frac{\partial^2 U_i}{\partial x_k^2}\frac{\partial^2 U_i}{\partial x_j^2}}; \quad U' = \sqrt{2\cdot S_{ij}S_{ij}} \quad (2)$$

In addition, a high wave number damping is used in the model to avoid accumulation of energy at the smallest scales. This is achieved by imposing a lower limit of the von Karman length scale:

$$L_{vK} = \max\left(\kappa\left|\frac{U'}{U''}\right|; C_S\sqrt{\frac{\kappa\zeta_2}{\beta/c_\mu - \alpha}}\Delta\right); \quad \Delta = \sqrt[3]{V} \quad (3)$$

with $C_s=0.11$, $\kappa=0.41$, $c_\mu=0.09$ and $\alpha=0.44, \beta=0.0828$ are the k-ε related coefficients of the SST model.

2.2 Forcing Terms for the SAS-F Model

Forcing terms are introduced into the momentum equations for modelling the transfer of modelled to resolved turbulent kinetic energy. In addition, a sink term is defined for the equation of the modelled turbulent kinetic energy, k, in order to preserve the energy between the resolved and modelled portions. The source terms read:

$$F_{mom,i} = \frac{\rho u_{f,i}}{\Delta t}; \qquad F_k = -0.5\frac{\rho u_{f,i}^2}{\Delta t} \quad (4)$$

where ρ is the density, Δt the time step and u_{fi} the velocity fluctuation to be transferred. The velocity fluctuations are produced by using the Random Flow Generator (RFG) as proposed by Kraichnan (1969) and including modification of Batten et al. (2004) for the frequency distribution. The formulation is local and requires as input only the length and time scale of the RANS turbulence model:

$$u_{f,i} = \sqrt{\frac{2}{3}k}\cdot\sqrt{\frac{2}{N}}\sum_{n=1}^{N}\left[p_i^n\cdot\cos\left(\arg^n\right)+q_i^n\cdot\sin\left(\arg^n\right)\right] \quad (5)$$

$$p_i^n = \varepsilon_{ijk}\eta_j^n d_k^n, \quad q_i^n = \varepsilon_{ijk}\xi_j^n d_k^n$$

$$\arg^n = 2\pi\left(\frac{d_i^n x_i}{L_t}+\frac{\omega^n t}{\tau_t}\right)$$

where $L_t = C_L \frac{\sqrt{k}}{C_\mu \omega}, \quad (C_L = 0.5)$ is the length scale of turbulence and $\tau_t = \frac{L_t}{\sqrt{k}}$ the time scale.

$$\eta_i^n = N(0,1), \quad \xi_i^n = N(0,1), \quad d_i^n = N(0,0.5), \quad \omega^n = N(1,1) \tag{6}$$

N(φ, ψ) is a normally distributed random variable with mean *φ* and standard deviation *ψ*. Numerical experiments have shown that typically *N~200* modes are sufficient for the required energy transfer. Furthermore, it is not sensible to transfer energy of modes which cannot be resolved with a given numerical grid and time step. A Nyquist limiter is therefore employed:

$$\frac{\tau_t}{\omega^n} \geq 2 \cdot \Delta t; \quad \frac{L_t}{|d^n|} \geq 2 \cdot \Delta h \tag{7}$$

where $|d^n| = \sqrt{d_i^n d_i^n}$ is the magnitude of the wave number, $\Delta \mathrm{h} = \max(\Delta_x, \Delta_y, \Delta_z)$ is the characteristic cell size. Note that an isotropy assumption is used instead of the Cholesky decomposition in the formulation of the RFG. This is deemed sufficient for these first tests. It should also be noted that there is a dynamic interaction between the SAS turbulence model and the RFG, as the SAS model adjust automatically to the smallest resolved scales. As these scales are typically in the LES-limit, the assumption of isotropic turbulence seems justified.

3 Numerical Method

The simulations have been carried out with the general purpose CFD code ANSYS Fluent 12.0. The RFG model has been implemented via a User Defined Function (UDF). The code is based on a cell-centred finite volume method for unstructured hybrid grids. In the current simulations, the pressure-based incompressible option in the solver has been selected. For the spatial discretization of the momentum equations, a pure central differencing scheme of second order accuracy was applied, whereas for the turbulence equations a second order upwind scheme was used. A second-order implicit scheme was chosen for time integration, and a non-iterative time-advancement (NITA) scheme (see, for ex., Armsfield & Street, 1999) was utilized to solve the equations at each time step.

4 Testcases

4.1 Decaying Isotropic Turbulence (DIT)

DIT is typically a test used for the calibration of LES models. In this mode, an initial resolved velocity field is generated in a box of dimension $2\pi \times 2\pi \times 2\pi$ and the decay of the resolved kinetic energy inside the box is tracked in time. In addition, spectral information is extracted through FFT and compared with experimental data. It is important to note that with the SAS model, the DIT case can be run in two modes. The first is the RANS mode, where only 2 values are specified for k and ω (or L_t and τ) and their variation in time is computed (from the k- and ω–equation). However, as the SAS model can adjust to resolved scales, the model can also be run in ”LES” mode. In this mode, an initial resolved velocity field is specified and the turbulence model is run on that frozen field to convergence in order to generate initial conditions for k and ω. Once the turbulence level are established, the SAS model is run in combination with the momentum equations to produce a dynamically changing and decaying velocity distribution, like in the LES case. The SAS model is calibrated for achieving correct spectral information in this mode (see Figure 1).

In the current application, another mode is of interest, whereby no resolved velocity field is specified initially, but only two variables for k and ω are given as in the RANS simulation. However, using the RFG, the goal is the conversion of the unresolved turbulent kinetic energy into a resolved part and a remaining modelled portion (subgrid). In other words, the specified values of k and ω will be used in RFG for switching from RANS to “LES” mode. The RFG formulation is such that this transfer takes place essentially in the first time step. While the RFG forcing remains active also for the remainder of the simulation, its effect is substantially reduced due to the resulting small length scale and the activation of the Nyquist limiter.

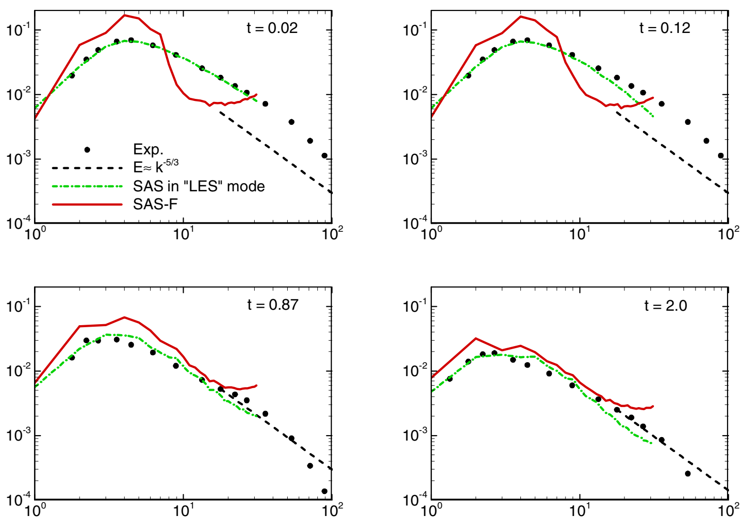

Fig. 1 Spectral development for Decaying Isotropic Turbulence (DIT) test case

Figure 1 shows the spectral development at 4 non-dimensional time values for the Compte-Bellot & Corrsin, (1971) experiment for a 64×64×64 grid. A time step of $\Delta t=0.005$ was used. Again, it has to be emphasized that the simulation is started with only two numbers: $k= 0.81$, $\omega=3.75$ and the entire spectral content is generated through the forcing terms and the RFG.

As expected, the initial spectrum generated by the RFG is not in perfect agreement when compared with the experimental data. Also, the behaviour at the high wave numbers is currently not fully understood. Nevertheless, the energy is successfully transferred from the modelled to the resolved part and the spectral distribution improves with time once the process is controlled by the momentum equations and the eddy-viscosity provided by the SAS model. Note that the turn-up of the energy at high wave numbers is a result of the RFG as can be seen in comparison with the SAS simulations starting from a resolved field ("LES" mode).

Figure 2 shows the strength of the RFG terms in the *k*-equation for the duration of the simulation. It is clear that the transfer of energy takes place essentially at the first time step, as designed (note logarithmic scale).

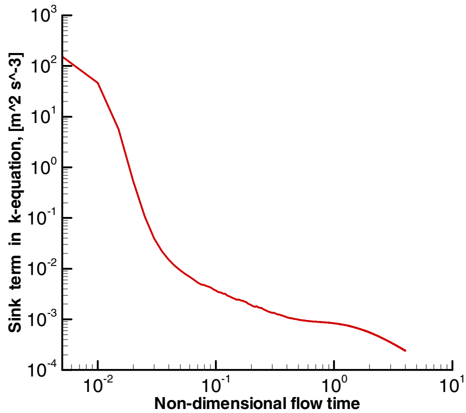

Fig. 2 Evolution of RFG sink term in the k-equation for the DIT test case

4.2 2D Channel Flow

The goal of the current formulation is to enable the SAS model to operate in unsteady mode even for flows which are URANS-stable. This applies to essentially all wall bounded flows (boundary layers, channel flows, …). While it is often desirable that the SAS model returns a RANS solution in such portions of the flow domain, there can be situations, where the switch to an unsteady formulation is desirable (for increased accuracy, for capturing unsteady effects further downstream, for acoustics simulations, etc.). The most widely used testcases for LES models in wall bounded flows are periodic turbulent channel flows at different Reynolds numbers. These flows reveal the essential weakness of LES models requiring substantial increases in grid resolution with Reynolds number. The current application of the SAS-F model to this flow is a first test for investigating the general behaviour of this concept and exploring the Reynolds number scaling on under-resolved grids. Four different Reynolds numbers (Re_τ=*395, 950, 2000* and *20 000*) have been computed without any adjustment/optimization of the model formulation. Table 1 shows the non-dimensional resolution for the four cases and also the number of nodes in streamwise, wall normal and spanwise direction. The time step used was $\Delta t=0.02$ and in the averaging procedure over 10 000 time steps were used.

Table 1 Non-dimensional grid resolution and grid dimensions for the channel flows.

Re_τ	*395*	*950*	*2000*	*20 000*
N_x	73	81	81	81
N_y	75	97	97	141
N_z	73	61	61	61
Δx^+	35	100	200	2000
Δy^+	30	50	100	1000
Δz^+	17	50	100	1000

Figure 3 shows the turbulent structures computed with the SAS-F model for the four Reynolds numbers depicting iso-surfaces of $Q=S^2\text{-}W^2$ ($Q_{iso}=0.3$).

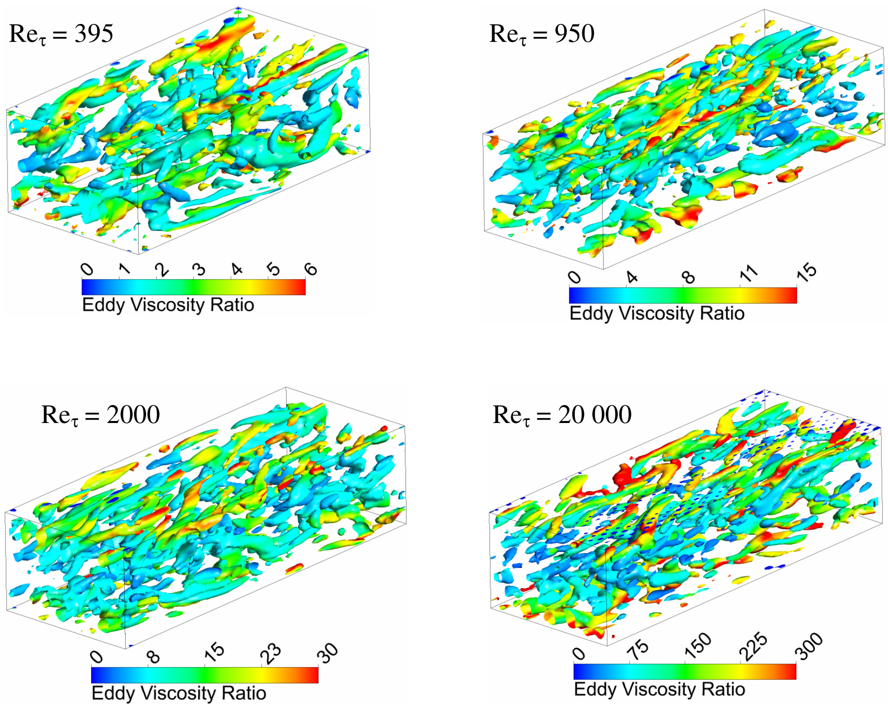

Fig. 3 Turbulent structures in developed channel flow computed with the SAS-F model for the four Reynolds numbers. Iso-surfaces correspond to the value of Q-invariant equal to 0.3 for all the cases, coloured with (eddy viscosity/molecular viscosity) ratio

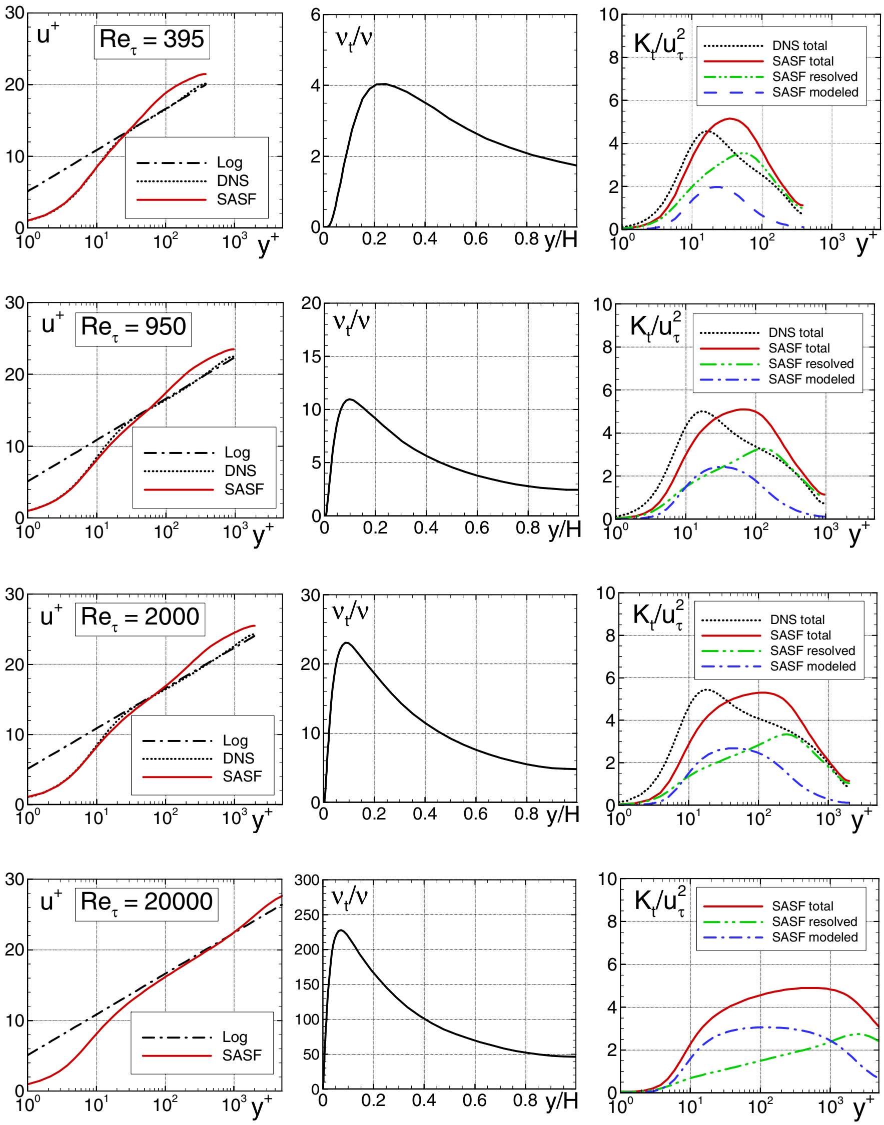

Fig. 4 Velocity profiles in wall-coordinates and eddy viscosity ratio across the channel for the four Reynolds numbers computed using the SAS-F model

Figure 4 shows the non-dimensional velocity profiles along with the corresponding profiles of the eddy-viscosity. It can be seen that the velocity profiles lay above the DNS and the desired Log profile. In addition, the model shows a double layer structure for the high Re number (and thereby under-resolved) cases similar to the profiles obtained with DES-hybrid models if no additional modifications are applied. While this is not an optimal behaviour, it is considered an encouraging starting point for the formulation of a more sophisticated model for such flows. It also appears that the simulations actually improve with higher Reynolds number. This behaviour and possible enhancements of the model will be explored in the future.

4.3 Backward Facing Step Flow

The backstep flow is an interesting practical candidate for the SAS-F model. Again the flow is stable when run with the SST-SAS model. It is however anticipated that the flow can be converted to unsteady mode with less impact of the forcing terms than for the channel flow. The reason lies in the shear layer emanating from the step. This layer is less stable than an attached boundary layer and will be able to quickly dominate the approximations of the RFG method, once unsteady structures appear. The situation for the backstep is actually more relevant for industrial flow simulations, than the channel flow. In engineering flows, it is often more desirable to resolve parts of the turbulent spectrum in separated flows, than to resolve the actual wall boundary layer.

In the current test, the experiment of Vogel & Eaton, 1985 is computed. The Reynolds number based on the step height is 28 000. Inlet profiles are specified from the experiment. The simulation is carried out on a grid of 2,309,715 nodes. A fragment illustrating the grid in the XY plane is shown in Figure 5. In the spanwise direction, the grid has 81 nodes and the domain size is Z/H = 4. The time step was Δt=0.02 and 5 000 time steps where accumulated in the averaging of the flow. The forcing terms are activated only downstream of the step.

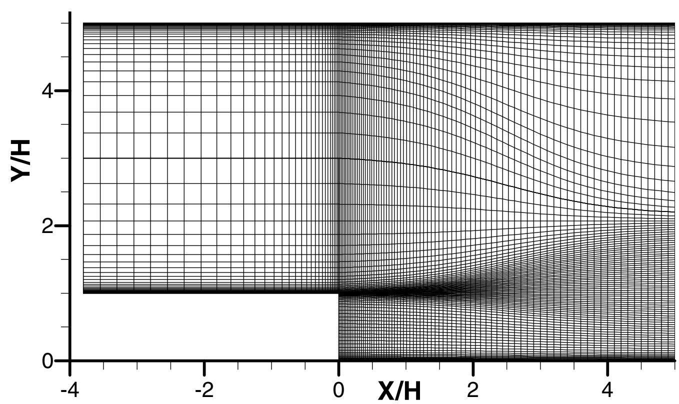

Fig. 5 Fragment of the grid for the backward-facing step in the XY plane

Figure 6 shows the turbulent structures again using an iso-surface of the Q-criterion ($Q_{iso}=0.5$). One can clearly see the flow instability emanating from the step. The effect of the RFG is actually relatively small in this flow, and is quickly dominated by the flow instability (note that RFG generates isotropic turbulent structures, contrary to the observed structures in Figure 6).

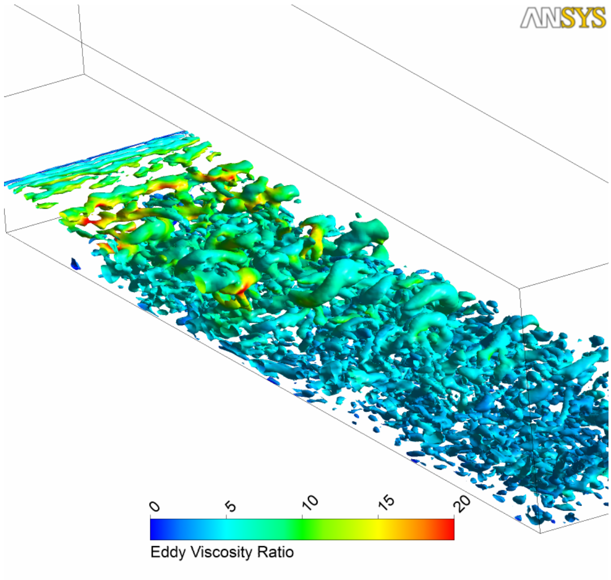

Fig. 6 Turbulent structures in the backward-facing step flow computed with the SAS-F model. Iso-surface of the Q-invariant = 0.5 colored with eddy viscosity ratio

Figure 7 shows the wall shear stress distribution downstream of the step. It is in good agreement with the experimental data, giving the correct flow reversal and reattachment location. The C_f in the recovery region downstream of reattachment is still low compared to the data. This was however also observed in pure LES simulations. An alternative set of experimental data indicates lower values – this will have to be explored in more detail.

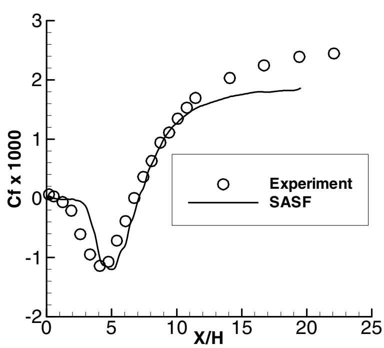

Fig. 7 Distribution of skin friction coefficient downstream of the backward-facing step. Result from the SAS-F model is averaged in time and in spanwise direction

Figure 8 shows a comparison of the velocity profiles. Again, the agreement with the data is quite good considering the early development status of the model.

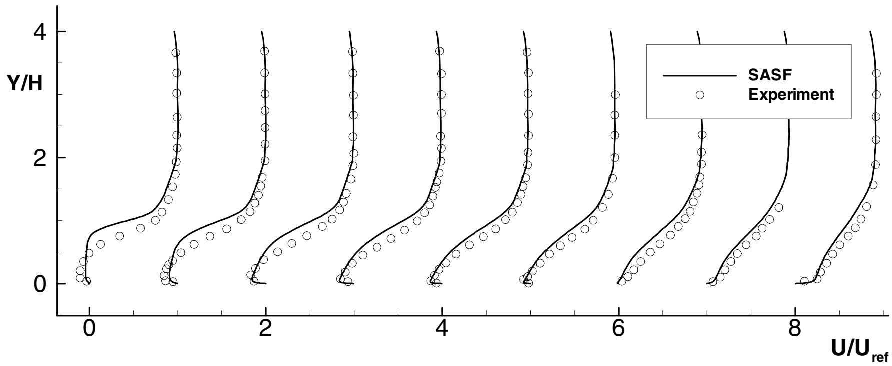

Fig. 8 Mean profiles of the streamwise velocity downstream of the backward-facing step. Results from the SAS-F model are averaged in time and in spanwise direction

5 Summary

Forcing terms for the SST-SAS model have been proposed. They allow the model to switch to unsteady mode even if the flow is stable for the conventional SST-SAS model. The forcing terms can be activated in limited regions of the domain and allow a convenient selection of the unsteady flow regime. The SST-SAS-F model has been applied in this first iteration to three testcases and has shown an overall good performance, considering that no optimization of the formulation has been attempted to capture additional effects as e.g. in wall bounded flows. The model will be developed further within the European Research project ATAAC.

Acknowledgement. The original SST-SAS model has been developed partly within the EU research project DESIDER (Detached Eddy Simulation for Industrial Aerodynamics) under contract No. AST3-CT-200-502842 (http://cfd.mace.manchester.ac.uk/desider/)

References

Armsfield, S., Street, R.: The Fractional-Step Method for the Navier-Stokes Equations on Staggered Grids: Accuracy of Three Variations. Journal of Computational Physics 153, 660–665 (1999)

Batten, P., Goldberg, U., Chakravarty, S.: Interfacing statistical turbulence closures with large-eddy simulation. AIAA Journal 42, 485–492 (2004)

Compte-Bellot, G., Corrsin, S.: Simple Eulerian time correlation of full – and narrow band velocity signals in grid-generated, “isotropic” turbulence. J. Fluid Mech. 48, 273–337 (1971)

Davidson, L.: Evaluation of the SST-SAS Model: Channel Flow, Asymmetric Diffuser and Axi-symmetric Hill. In: Proc. ECCOMAS CFD 2006 (2006)

Grahs, T., Othmer, C.: Evaluation of Aerodynamic Noise Generation: Parameter Study of a Generic Side Mirror Evaluating the Aeroacoustic Source Strength. In: Proc. ECCOMAS CFD (2006)

Kraichnan, R.H.: Diffusion by a random velocity field. Phys. of Fluids 13(1), 22–31 (1969)

Menter, F.R.: Two-Equation Eddy-Viscosity Turbulence Models for Engineering Applications. AIAA-Journal 32(8), 269–289 (1994)

Menter, F.R., Egorov, Y.: Re-visiting the turbulent scale equation. In: Proc. IUTAM Symp. One Hundred Years of Boundary Layer Research, Göttingen. Springer, Heidelberg (2004/2006)

Menter, F.R., Egorov, Y.: A Scale-Adaptive Simulation Model using Two-Equation Models, AIAA Paper 2005-1095, Reno/NV (2005a)

Menter, F.R., Egorov, Y.: Turbulence Models based on the Length-Scale Equation. In: Fourth International Symposium on Turbulent Shear Flow Phenomena, Williamsburg, 2005 – Paper TSFP4-268 (2005b)

Menter, F.R., Egorov, Y.: SAS Turbulence Modelling of Technical Flows. In: DLES 6 - 6th ERCOFTAC Workshop on Direct and Large Eddy Simulation September, Poitiers (2005c)

Menter, F.R., Egorov, Y., Rusch, D.: Steady and Unsteady Flow Modelling Using the $k-\sqrt{k}L$ Model. In: Hanjalic, K., Nagano, Y., Jakirlic, S. (eds.) Proc. Turbulence, Heat and Mass Transfer, vol. 5 (2006)

Rotta, J.C.: Turbulente Strömumgen. BG Teubner Stuttgart (1972)

Smirnov, A., Shi, S., Celik, I.B.: Random flow generation technique for large-eddy simulations and particle-dynamics modelling. J. of Fluids Engineering 123, 359–371 (2001)

Spalart, P.R.: Strategies for turbulence modelling and simulations. Int. J. Heat Fluid Flow 21, 252–263 (2000)

Vogel, J.C., Eaton, J.K.: Combined heat transfer and fluid dynamics measurements downstream of a backward-facing step. ASME J. Heat Transfer 107, 922–929 (1985)

Widenhorn, A., Noll, B., Aigner, M.: Numerical study of a non-reacting turbulent flow in a gas turbine model combustor, AIAA Paper, AIAA 2009-647, Orlando (2009)